SOIL, 11, 793–809, 2025
https://doi.org/10.5194/soil-11-793-2025

SOIL Open Access EGU

High biodegradability of water-soluble organic carbon in soils at the southern margin of the boreal forest

Yuqi Zhu[1,2], Chao Liu[3], Rui Liu[1,2], Hanxi Wang[1,2], Xiangwen Wu[1,2], Zihao Zhang[1,2], Shuying Zang[1,2], and Xiaodong Wu[1,2,4]

[1]Heilongjiang Province Key Laboratory of Geographical Environment Monitoring and Spatial Information Service in Cold Regions, Harbin Normal University, Harbin 150025, China
[2]Heilongjiang Province Collaborative Innovation Center of Cold Region Ecological Safety, Harbin 150025, China
[3]School of Resources and Environment, Northeast Agricultural University, Harbin 150030, China
[4]Cryosphere Research Station on Qinghai-Tibet Plateau, State Key Laboratory of Cryospheric Science and Frozen Soil Engineering, Northwest Institute of Eco-Environment and Resources, Chinese Academy of Sciences, Lanzhou 730020, China

Correspondence: Shuying Zang (zsy6311@hrbnu.edu.cn) and Xiaodong Wu (wuxd@lzb.ac.cn)

Received: 12 January 2025 – Discussion started: 7 February 2025
Revised: 24 July 2025 – Accepted: 12 August 2025 – Published: 9 October 2025

Abstract. Water-soluble organic carbon (WSOC) is an important component of the soil organic carbon pool. While the biodegradability and its compositional changes of WSOC in deep soils in boreal forests remain unknown. Here, based on spectroscopic techniques, we conducted a 28 d laboratory incubation to analyze the molecular composition, biodegradability, and compositional changes of WSOC during a laboratory incubation for deep soils at the southern boreal margin. The results showed that in the upper 2 m soils, the average content of biodegradable WSOC was 0.228 g kg^{-1} with an average proportion of 86.41 % in the total WSOC. In the soil layer between 2.0–7.4 m, the average biodegradable WSOC content was 0.144 g kg^{-1}, accounting for 80.79 % of the total WSOC. Spectroscopic analysis indicates that the WSOC in the upper soils is primarily composed of highly aromatic humic acid-like matter with larger molecular weights than those in deep soils. Both the aromaticity and molecular weight decrease with depth, and the WSOC is mainly composed of fulvic acid-like matter in the deep soils, suggesting high biodegradability of WSOC in the deep soils. Overall, our results suggest that the water-soluble organic carbon in the boreal forests exhibits high biodegradability both in the shallow layer and deep soils.

1 Introduction

Boreal forests cover only around 11 % of Earth's land surface, while they store one-third of the global terrestrial carbon stock (Adamczyk, 2021), and substantial amounts are also present in deep layers (Bockheim and Hinkel, 2007; Strauss et al., 2017; Schirrmeister et al., 2011). Climate change can influence carbon release and sequestration in these soils (Ohlson et al., 2009; Liang et al., 2024), for example, through the melting of ground ice, the occurrence of wildfires, and rising soil temperatures (Zhong et al., 2023; Gao et al., 2021; Zhang et al., 2023; Bond-Lamberty et al., 2007; Kasischke et al., 1995). These changes also alter the composition of soil microbial communities, affecting their stability and functional capacity, and ultimately leading to the loss of organic carbon in northern ecosystems (Zhong et al., 2023; Wu et al., 2021).

Water-soluble organic carbon (WSOC) is a complex mixture composed of both high- and low-molecular-weight compounds, derived from vegetation, litter, root exudates, and microbial biomass and enzymes (Thurman, 1985; Guggenberger and Zech, 1994). It serves as an important sub-

strate for microbial activity (Neff and Asner, 2001; Moore, 2003). Biodegradable WSOC (BWSOC) denotes the portion of water-soluble organic carbon that can be utilized and metabolized by microorganisms (Khan et al., 1998; Marschner and Kalbitz, 2003; Scaglia and Adani, 2009; Vonk et al., 2015). The bioavailability of WSOC largely depends on its chemical composition: simple organic compounds such as amino acids, carbohydrates, and fatty acids are more easily decomposed, whereas more complex components like humic substances require longer decomposition times (Ma et al., 2019). Most leachates from litter and vegetation are dominated by low-molecular-weight molecules, which are highly biodegradable and support microbial growth (Michalzik et al., 2003). Although WSOC accounts for only about 1 % of soil organic carbon (SOC) (Margesin, 2008), it represents the most mobile and bioavailable fraction of SOC (Kaiser and Kalbitz, 2012). Climate change can enhance the release of soil carbon as dissolved organic carbon (DOC) into surface water (Bowden et al., 2008; Olefeldt and Roulet, 2012). Understanding the dynamics of this carbon fraction is critical for elucidating SOC turnover in boreal forests (Olefeldt et al., 2014; Öquist et al., 2014).

Due to the cold temperatures, the decomposition rate of soil organic matter (SOM) in boreal forests is low due to the low soil microbial activity (Walz et al., 2017). Over millennial timescales, frozen conditions and cryopedogenic processes, such as cryoturbation, have buried organic-rich surface soils into deep layers, further reducing decomposition rates and promoting long-term carbon sequestration (Ping et al., 2015). These low decomposition rates result in a high proportion of labile and biodegradable fractions within soil organic carbon in boreal forests (Song et al., 2020), including water-soluble organic carbon (Cory et al., 2013). Studies indicate that WSOC in shallow boreal forest soils is highly biodegradable (Panneer Selvam et al., 2016), with its bioavailability ranging from 24 % to 71 % (Ma et al., 2019). However, most of the previous studies focused on WSOC in runoff or soil water rather than in situ conditions, leaving significant knowledge gaps that hinder our ability to predict SOC loss under a warming climate.

Previous studies in permafrost regions showed that several factors can significantly influence the concentration, aromaticity, molecular weight, and optical characteristics of dissolved organic matter (DOM) (Kurashev et al., 2024). For instance, a freeze–thaw manipulation in a continuous permafrost region of northern Sweden showed that WSOC biodegradability increased as the freezing front deepened, largely because protein-like compounds accumulated at this depth (Panneer Selvam et al., 2016). The chemical nature of WEOM can be an important factor affecting the decomposition of SOM (Paré and Bedard-Haughn, 2013). In addition, hydrological-redox status can jointly control the stability of SOM (Pengerud et al., 2013). The tabular ground ice contains a high proportion of labile DOC that may accelerate the decomposition of permafrost SOM during melting (Semenov et al., 2024). These studies improved our understandings of DOM in permafrost regions, while few studies have been conducted in the southern boundary area of boreal forest, which may represent the future conditions of vast boreal forests due to the climate warming.

Many studies have been conducted to reveal the SOM characteristics within 3 m soils. In a 0–3 m permafrost profile in the Kolyma River Basin in Siberia, it was found that SOM in permafrost contain more water-soluble substrates and, after thaw, can be rapidly degraded by active microbes (Uhlířová et al., 2007). In a Northeast Siberia area, the active layer in around 60 cm, and it was found that the SOM from permafrost within 1 m depth was more sensitive to temperature changes than that of active layer (Walz et al., 2017). Since soil deep than 3 m in permafrost regions constitute a large proportion of permafrost carbon pools, and this carbon pool may also contribute to the future soil organic carbon cycle (Schuur et al., 2022), it is necessary to understand the SOM dynamics deeper than 3 m depth.

Microorganisms play a key role in the carbon cycle and strongly influence the biodegradability of WSOC (Marschner and Kalbitz, 2003; Kalbitz et al., 2003a; Neff and Asner, 2001; Yano et al., 2000). Microbial biomass is more abundant in surface horizons, where soil-organic-carbon mineralization proceeds rapidly (Henneron et al., 2022; Pei et al., 2025), whereas thaw-activated bacteria in deeper layers can rapidly mineralize WSOC after permafrost thaws (Drake et al., 2015). Microbial use of WSOC is modulated by environmental factors such as soil moisture (Zhang et al., 2024; Li et al., 2020) and soil physicochemical properties (Lv et al., 2024; Shao et al., 2022a). Therefore, detailed knowledge of the content, chemical composition, and biodegradability of WSOC along deep soil profiles is critical for clarifying how subsurface carbon is mobilized, transformed, and ultimately influences carbon cycling in boreal forests. The objective of this study is to quantify WSOC of soil profile that deeper than 3 m in a southern boreal margin. We conducted laboratory incubation experiments to determine differences in biodegradable water-soluble organic carbon (BWSOC) and employed spectroscopic techniques to reveal its compositional characteristics (Kothawala et al., 2014; Chavez-Vergara et al., 2014; Sun et al., 2022; Murphy et al., 2008; He et al., 2023). The results can improve our understandings of SOC in boreal forests under a warming climate.

2 Materials and methods

2.1 Study area and sample collection

The southern region of the boreal forest is highly sensitive to climate warming (Randerson et al., 2006; Zou and Yoshino, 2017; Peng et al., 2022). The forests of the Daxing'an Mountains in Northeast China represent the southernmost extent of the boreal forest biome (Jiang et al., 2002; Huang et al., 2010). The sampling site (50°24′10.8″ N, 120°50′12.9″ E)

Table 1. Depths, soil colors (Munsell color system), textures (based on "texture-by-feel" estimation) of soil samples.

Named	Depth	Soil color	Soil texture
L1	0–10 cm	10YR 2/1	Heavy loam
L2	10–20 cm	10YR 2/1	Heavy loam
L3	20–30 cm	10YR 2/1	Heavy loam
L4	30–60 cm	7.5YR 2.5/1	Silty clay Loam
L5	60–90 cm	7.5YR 2.5/1	Silty clay Loam
L6	90–120 cm	7.5YR 2.5/1	Silty clay Loam
L7	120–150 cm	7.5YR 2.5/1	Silty clay Loam
L8	150–160 cm	7.5YR 2.5/1	Silty clay Loam
L9	160–180 cm	7.5YR 2.5/1	Silty clay Loam
L10	220–250 cm	7.5YR 5/2	Silty clay Loam
L11	420–450 cm	10YR 4/3	Sandy clay
L12	700–740 cm	10YR 4/3	Sandy clay

is located within the island permafrost zone (Bockheim, 2006; Ran et al., 2012; Brown et al., 1997) (Fig. 1). In 2023, the mean average temperature was −1.24 °C, and the annual precipitation of 290.3 mm (Qweather, https://www.qweather.com/en/historical/ergun-101081014.html, last access: 13 September 2025). The dominant tree species in the study area is *Betula platyphylla*, which characterizes the typical local forest ecosystem (Zou and Yoshino, 2017; Jiang et al., 2002).

During 9–11 July 2023, a soil column (13.5 cm in diameter) was collected from a piedmont terrace at an elevation of 734 m. The column extended to a depth of 740 cm and was divided into 12 layers (L1–L12). Soil texture was determined in the field using the "texture-by-feel" estimation method (Vos et al., 2016). Soil color was recorded using the Munsell Soil Color Chart (Table 1). There is structural ice in at the depth between 160–180 cm. Although we could not verify whether this area has permafrost because we lack the ground monitoring data, this site represents the southern margin of the boreal forests.

2.2 Physicochemical analysis and spectral analysis of WSOC

Gravimetric soil moisture (GSM) was quantified using the gravimetric method (Reynolds, 1970). Soil pH was measured with a PHS-3E pH meter (Leici, China) after shaking a soil-water suspension at a ratio of 1 : 2.5 (w/v). Soil electrical conductivity (EC) was determined using a DDSJ-319L conductivity meter (Leici, China) with a soil-to-water ratio of 1 : 5 (w/v). Soil organic carbon (SOC) and total carbon (TC) contents were determined by the dry combustion method using a Multi N/C 3100 analyzer (Jena, Germany) (Nelson and Sommers, 1996); the TC and SOC samples were first air-dried. Before SOC determination, approximately 100 mg of sample was weighed into a ceramic boat, an excess of 4 mol L^{-1} HCl was added until no bubbles evolved, the mixture was thoroughly homogenized and left to stand for 4 h, and then dried at 65 °C for 16 h prior to analysis. Soil inorganic carbon (SIC) was calculated through differential subtraction.

Water-soluble organic carbon (WSOC) was extracted by adding fresh soil samples sieved through a 2 mm sieve, to deionized water at a ratio of 1 : 5 (w/v). The mixture was shaken continuously for 4 h at 200 r min^{-1} and 25 °C. The samples were then centrifuged for 15 min at 4500 r min^{-1} and filtered through 0.45 µm glass fiber filters (Jones and Willett, 2006). A portion of the filtrate was used for ultraviolet spectroscopic analysis, and the remaining filtrate was acidified by adding 3 mol L^{-1} hydrochloric acid to adjust the pH to ≤ 2, effectively removing inorganic carbon. The pretreated samples were stored at 4 °C and analyzed within a week using the dry combustion method with a Multi N/C 3100 analyzer (Jena, Germany).

Total nitrogen (TN) was converted into ammonium nitrogen through an oxidation-reduction reaction under the influence of concentrated sulfuric acid, sodium thiosulfate, and a catalyst (Kirk, 1950), and quantified using the ammonia nitrogen module of a SAN++ flow injection auto-analyzer (Skalar, Holland). Ammonium nitrogen (NH_4^+-N) and nitrate nitrogen (NO_3^--N) were determined after extracting 2 g of fresh soil into 10 mL of 2 mol L^{-1} potassium chloride solution, shaking for 2 h at 200 r min^{-1}, then centrifuging for 3 min at 8000 r min^{-1} and filtering through 0.45 µm glass fiber filters (Li et al., 2012).

Total phosphorus (TP) in soil was determined using sodium hydroxide to convert all phosphorus-containing minerals and organic phosphorus compounds into soluble orthophosphates (Sparks et al., 2020), which were then quantified using a SAN++ flow injection auto-analyzer (Skalar, Holland).

Different WSOC compounds exhibit distinct spectral properties, and ultraviolet-visible (UV-Vis) absorption spectra are commonly used to assess WSOC quality. The absorbance at 254 nm ($SUVA_{254}$) is strongly correlated with WSOC aromaticity (Weishaar et al., 2003b). The *E250 / E365* ratio, indicative of WSOC aromaticity, humification degree, and molecular size (Helms et al., 2008), is also an important parameter for characterizing WSOC. The absorbance values of WSOC at 250, 254, and 365 nm were measured using a Lambda 35 UV/VIS spectrometer (PerkinElmer, USA) with a 10 mm quartz cuvette. For each sample, the $SUVA_{254}$ value was calculated by dividing the UV absorbance measured at 254 nm by the WSOC concentration and multiplying 100 (Weishaar et al., 2003a). The *E250 / E365* ratio was obtained by dividing the absorbance value at 250 nm by that at 365 nm (Helms et al., 2008). Throughout the incubation period, including the initial measurement on Day 0, UV-Vis spectroscopy was conducted on a portion of the WSOC extract to assess quality parameters such as $SUVA_{254}$ and the *E250 / E365* ratio.

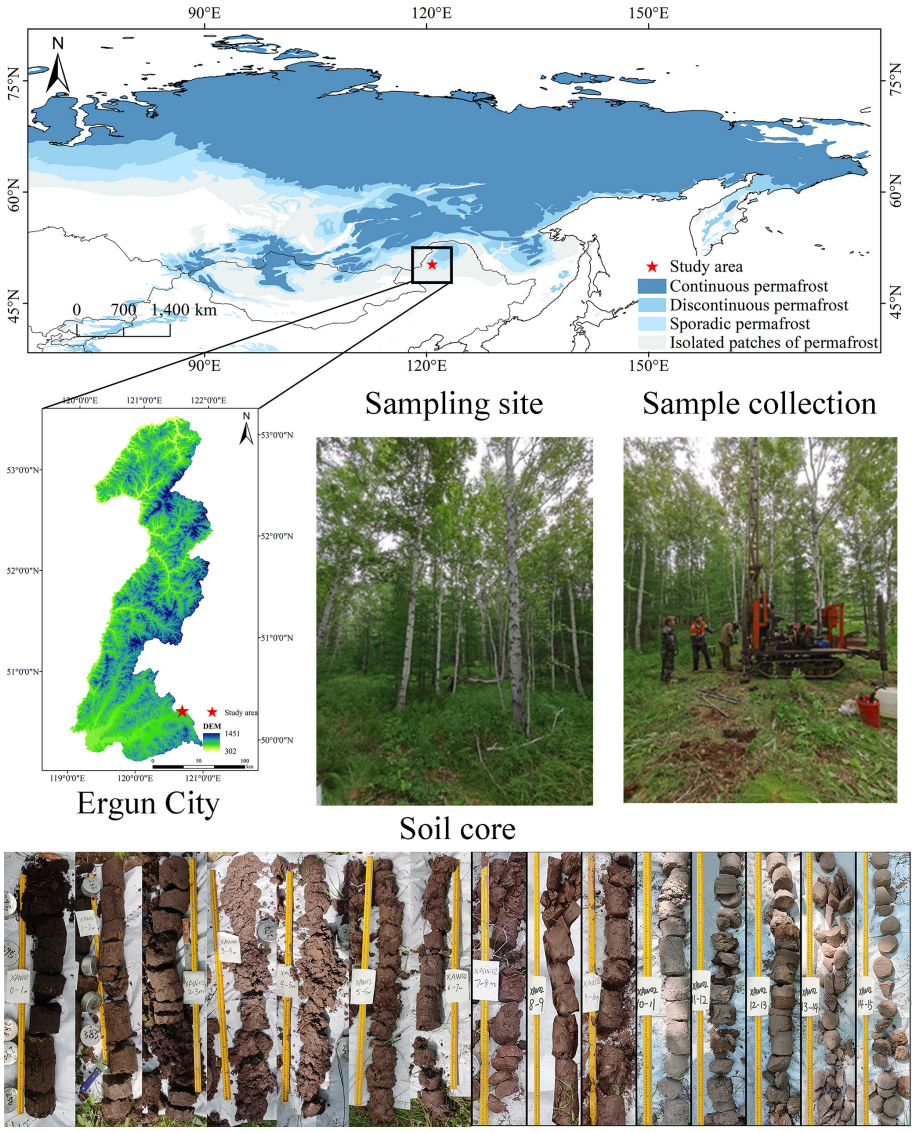

Figure 1. Study area and soil core sample collection. Permafrost distribution is adapted from Circum-Arctic map of permafrost and ground ice condition (Brown et al., 1997).

The $SUVA_{254}$ and the *E250 / E365* ratio are widely used but semi-quantitative indicators. $SUVA_{254}$ can be inflated by non-aromatic UV-absorbers such as nitrate and dissolved Fe(III) and cannot distinguish among different aromatic moieties (Weishaar et al., 2003b; Logozzo et al., 2022). The *E250 / E365* ratio provides only a coarse estimate of mean chromophore size; it is sensitive to baseline drift, light scattering, and becomes unreliable at low absorbance (Peuravuori and Pihlaja, 2004). By contrast, excitation–emission matrix (EEM) fluorescence spectroscopy yields multidimensional data with high sensitivity at low organic-matter concentrations (Anumol et al., 2015; Sgroi et al., 2018). In this study we therefore applied three-dimensional fluorescence spectroscopy to characterize water-extractable organic matter (WEOM). Fluorescence spectra were partitioned into five regions on the basis of integrated fluorescence area (Chen et al., 2003) (Table S1 in the Supplement). WEOM was extracted by adding deionized water to fresh soil samples sieved through a 2 mm sieve at a soil-to-water ratio of 1 : 5 (w/v), followed by shaking at 200 r min^{-1} for 24 h at 25 °C. The samples were then centrifuged at 4500 r min^{-1} for 15 min, and the supernatant was filtered through a 0.45 µm glass fiber filter to obtain WEOM (Zhou et al., 2023). A three-dimensional fluorescence spectrophotometer (Aqualog, HORIBA Scientific, France) was used to identify the fluorescent substances in water soluble organic matter. The excitation wavelength was set from 200 to 450 nm and the emission wavelength from 250 to 550 nm, with both the excitation and emission sampling intervals and slits adjusted to 5 nm, and the scanning speed maintained at 12 000 nm min^{-1}.

Because solute concentrations are lower in deeper-soil extracts, the extraction time for WEOM was extended relative to that for WSOC to obtain sufficient concentration and fluorescence signal (Zhou et al., 2023). Although a longer extraction can introduce minor compositional changes (Corvasce et al., 2006; Park and Snyder, 2018), EEM fluorescence nevertheless remains a robust method for assessing WSOC biodegradability (Vonk et al., 2015; Mu et al., 2017; Zhou et al., 2023).

2.3 Laboratory Incubation experiment

In the laboratory incubation experiments, we assessed the biodegradable water-soluble organic carbon (BWSOC) at various soil depths over a period of 28 d, with measurements of WSOC content taken on days 0, 2, 7, 14, and 28 (Vonk et al., 2015; Mu et al., 2017).

To minimize variability, WSOC samples were extracted in bulk from each soil layer. Fresh soil samples, sieved through a 2 mm sieve, were mixed with deionized water at a soil-to-water ratio of 1 : 5 (w/v), shaken continuously at 200 r min^{-1} and 25 °C for 4 h, centrifuged at 4500 r min^{-1} for 15 min, and filtered through 0.45 µm filters. The resulting WSOC solution (500 mL) from each soil layer was thoroughly homogenized. Aliquots of 30 mL of the homogenized WSOC solution were transferred into 50 mL sterile serum bottles.

To prepare the microbial inoculum, fresh soil samples from each soil layer were sieved through a 2 mm sieve to remove debris and large particles. The sieved soil was mixed with sterile deionized water at a ratio of 1 : 5 (w/v) and shaken continuously at 200 r min^{-1} and 25 °C for 4 h. This process facilitated the release of microorganisms from soil particles into the aqueous phase, allowing them to enter the extract in suspension form (Bottomley et al., 2020). The suspension was then centrifuged at 4500 r min^{-1} for 15 min to remove any remaining soil particles. The supernatant was filtered through pre-combusted (450 °C for over 4 h) Whatman GF/C filters with a pore size of 1.2 µm to obtain the microbial inoculum. Finally, 3 mL of the inoculum (constituting 10 % of the total volume) was added to the water samples to introduce indigenous soil microorganisms from the respective soil depths (Vonk et al., 2015). Inocula and WSOC samples were always matched by depth, preserving the natural microbe–substrate association that is critical for realistic assessments of WSOC bioavailability and degradation potential (Bhattacharyya et al., 2022; Pei et al., 2025).

To minimize nutrient limitations on microbial activity, standardized amounts of ammonium nitrate (NH_4NO_3) and dipotassium hydrogen phosphate (K_2HPO_4) were added to each sample. Specifically, a 0.02674 mol L^{-1} NH_4NO_3 stock solution was prepared by dissolving 2.14 g of NH_4NO_3 in 1 L of deionized water. Then, 100 µL of this stock solution was added to each 33 mL sample, resulting in final concentrations of approximately 80 µmol L^{-1} for NH_4^+ and NO_3^-. Similarly, a 0.0334 mol L^{-1} K_2HPO_4 solution was prepared by dissolving 5.8176 g of K_2HPO_4 in 1 L of deionized water, which was subsequently diluted tenfold to obtain a 0.00334 mol L^{-1} working solution. We added 100 µL of the diluted K_2HPO_4 solution to each sample, achieving a final PO_4^{3-} concentration of approximately 10 µmol L^{-1} (Mu et al., 2017; Vonk et al., 2015). Previous studies suggested that these additions are sufficient to prevent nutrient limitation and to standardize microbial activity (Mehring et al., 2013; Helton et al., 2015). By equalizing nutrient supply across soil layers, we attribute any differences in WSOC consumption to the intrinsic properties of the WSOC itself. Each sample was incubated in triplicate, along with two control blanks: one with deionized water and another with deionized water plus nutrients, for a total of five samples per depth interval. All samples were incubated at 20 °C in the dark in a constant temperature incubator (Thermo, USA), with caps partially opened. The samples were shaken once daily to maintain aerobic conditions.

On measurement days, the samples were re-filtered through a 0.45 µm glass fiber filter to exclude filterable microbial biomass. The quantified WSOC degradation accounted for both microbial mineralization and assimilation processes. Part of the samples was immediately used for absorbance measurements at wavelengths of 250, 254, and 365 nm. Another portion was acidified using 3 mol L^{-1} hydrochloric acid to adjust the pH to ≤ 2 and subsequently stored at 4 °C, with WSOC concentration measured within a week. BWSOC was determined by subtracting the WSOC content on day 28 from the WSOC content on day 0. BWSOC (%) was calculated by dividing BWSOC by the WSOC content on day 0 and multiplying by 100 %. The formulas for calculating BWSOC and BWSOC (%) are provided in the Supplement. All experimental procedures were conducted on a sterile laminar flow bench.

2.4 Data analysis

Pearson correlation analysis was used to explore the relationships between various environmental factors and characteristics of WSOC. One-way ANOVA was employed to test the significant differences in the molecular composition of WSOC, which was indicated by the $SUVA_{254}$ and *E250 / E365* ratios, across different soil depth. To compare the differences in biodegradable water-soluble organic carbon (BWSOC) across soil depths, the non-parametric Kruskal-Wallis test was applied. The biodegradability of water-soluble organic carbon at time ($BWSOC_t$) was underwent nonlinear exponential fitting to obtain the reaction kinetics constant (k). All statistical analyses were performed using R version 4.4.0 (https://www.r-project.org/, last access: 13 September 2025).

3 Results

3.1 Physicochemical properties

The concentration of nutrients in the soil gradually decreases with depth (Fig. 2). In the surface layer (0–30 cm), nitrogen content is lowest at the 10–20 cm depth. Electrical conductivity and total phosphorus content are highest at 700–740 cm. The WSOC content ranged from 0.123 to 0.355 g kg^{-1}. On average, WSOC content was 0.246 g kg^{-1} in the upper 0–2 m layer, while below 2 m it decreased to an average of 0.183 g kg^{-1}. The highest WSOC content, at 0.355 g kg^{-1}, was observed between 160–180 cm.

3.2 Spectroscopy of water-soluble organic carbon

There were significant differences in the aromaticity and molecular weight of WSOC between the 0–60 cm depth and deeper layers within the boreal forest ecosystem ($n = 3$, $p < 0.05$) (Fig. 3). The WSOC in the 0–60 cm depth predominantly consists of components with higher aromaticity and larger molecular weights. In contrast, deeper layers have WSOC with smaller molecular weights and less aromaticity (Fig. 3). Additionally, three-dimensional fluorescence spectroscopy displayed two major fluorescence peaks (Fig. 4): one in Region III, representing fulvic acid-like matter, and another in Region V, representing humic acid-like matter. The fluorescence intensity of fulvic acids is high across all depths, with significantly greater intensity in the 0–30 and 420–740 cm depths compared to other depths (Fig. 5).

3.3 Biodegradable water-soluble organic carbon, and the reaction kinetics constant *k*

BWSOC content and degradation kinetics exhibited pronounced, non-linear depth patterns (Fig. 6). Soils at 60–180 cm depth exhibited higher BWSOC content and degradability compared to other depths (Fig. 6). Significant variations in degradation rates were observed during the incubation process. The reaction kinetics constant (k values) indicated that WSOC degradation rates were lower in deeper soils (220–740 cm) (0.0681–0.0863 d^{-1}) (Table 2), mainly recorded between days 14 and 28 of incubation. In contrast, the WSOC at 60–90 cm depth decomposed faster during the early stages of incubation, with a k value of 1.0952 (d^{-1}). Although deeper soils (below 2 m) also contain relatively high BWSOC content, decomposition in these layers occurred primarily during the later stages of incubation (days 14–28), whereas the WSOC in upper layers (0–180 cm) was rapidly decomposed at the beginning of the incubation period (Fig. 7).

At 160–180 cm depth, $SUVA_{254}$ values gradually increased over the incubation period, while *E250 / E365* value steadily decreases (Fig. 8). This indicates that as the incubation time increases, the aromaticity and molecular weight of the remaining WSOC also increase. In contrast, WSOC at other depths is rapidly decomposed during the initial stages of incubation, leading to a quick increase in $SUVA_{254}$ and a rapid decrease in *E250 / E365* in the first 0–7 d, reflecting the rapid utilization of smaller, less aromatic molecules early in the incubation. The WSOC content at depths of 60–120 cm and the absorbance values at depths of 220–740 cm were extremely low by day 28, which likely resulted in very low $SUVA_{254}$ and *E250 / E365* values on that day. As a result, we excluded these data from the analysis.

3.4 Relationship among the biodegradation of water-soluble organic carbon and physicochemical parameters

Total carbon (TC), total nitrogen (TN), WSOC and its degradability showed significantly negative correlations with depth. The aromaticity of WSOC ($SUVA_{254}$) and molecular weight (*E250 / E365*) showed significant correlations with biodegradable water-soluble organic carbon (BWSOC). *E250 / E365* showed a positive correlation with BWSOC ($r = 0.528$), while $SUVA_{254}$ was negatively correlated with BWSOC ($r = -0.582$). Additionally, $SUVA_{254}$ and *E250 / E365* demonstrated a strong negative correlation ($r = -0.589$), suggesting that the molecular composition of WSOC significantly impacts its biodegradability. The degradation rate (k) and the degree of biodegradability (BWSOC%) of WSOC has no significant correlations with other physicochemical parameters (Fig. 9).

Simple-linear regressions showed that BWSOC declined with $SUVA_{254}$ ($\beta = -0.158 \pm 0.062$, $p = 0.029$, $R^2 = 0.395$) and increased with *E250 / E365* ($\beta = 0.003 \pm 0.001$, $p = 0.035$, $R^2 = 0.374$), whereas the degradation constant k was not significantly related to either index ($p \geq 0.05$) (Table S2, Fig. S1 in the Supplement). A multiple model including both optical variables accounted for 35 % of the variance in BWSOC (adjusted $R^2 = 0.350$, $p = 0.058$) but remained non-significant for k (adjusted $R^2 = 0.043$) (Tables S3 and S4, Fig. S2).

4 Discussion

4.1 Water-soluble organic carbon content and spectral signature

At depths of 60–180 cm, WSOC concentrations were relatively higher than in other soil layers. This pattern is plausible since higher organic matter inputs from roots and litter generally occur in these upper soil layers, facilitating WSOC accumulation (Hu et al., 2014). Additionally, the silty clay loam texture at these depths contains a substantial proportion of silt and clay particles, creating a denser pore structure capable of effectively adsorbing and retaining organic matter (Bucka et al., 2023). With increasing soil depth, the higher sand content can lead to lower porosity but higher macroporosity (Mentges et al., 2016). Consequently, higher sand

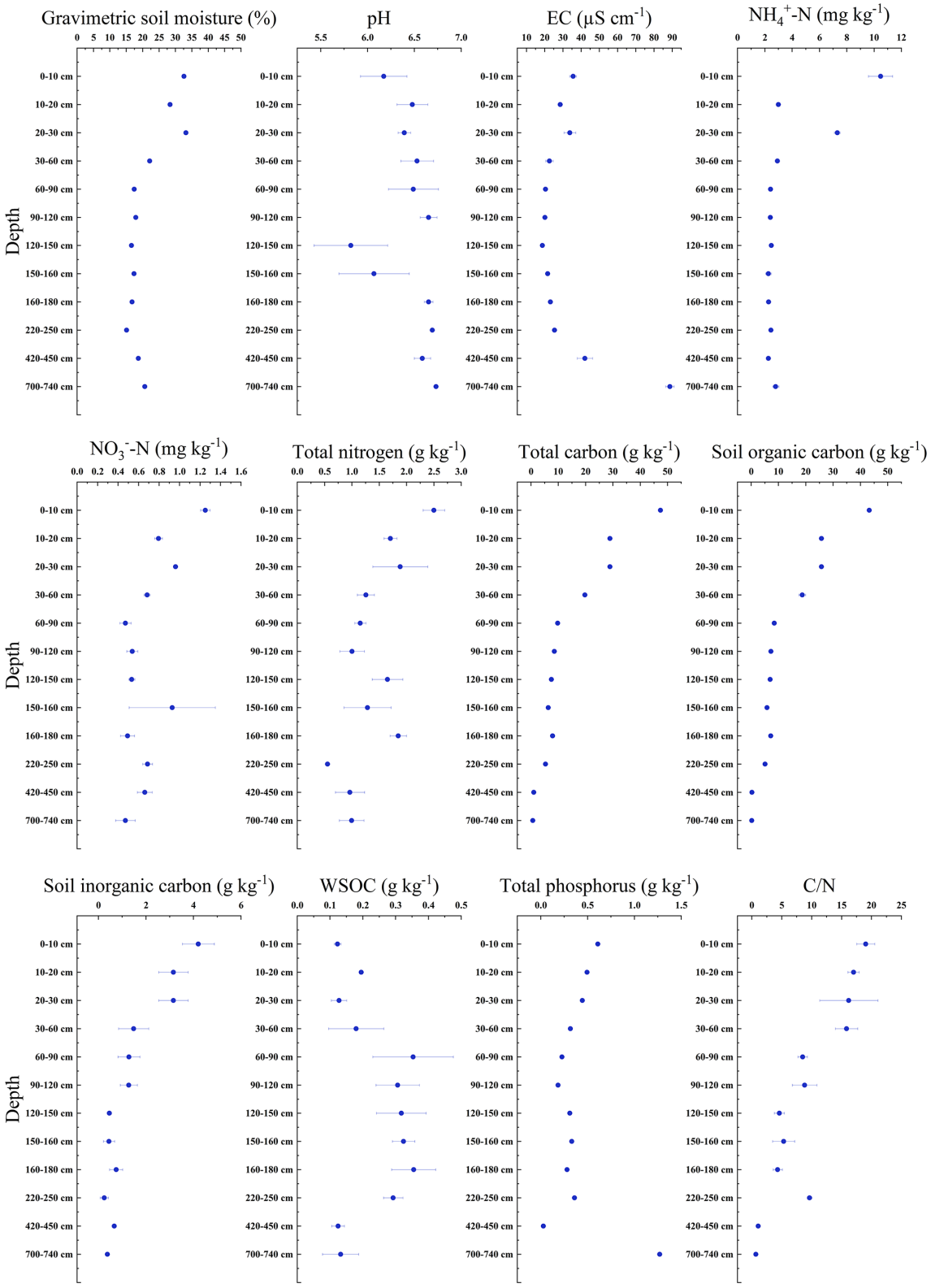

Figure 2. Soil physicochemical characteristics at different depth, error bars represent the standard error ($n = 3$).

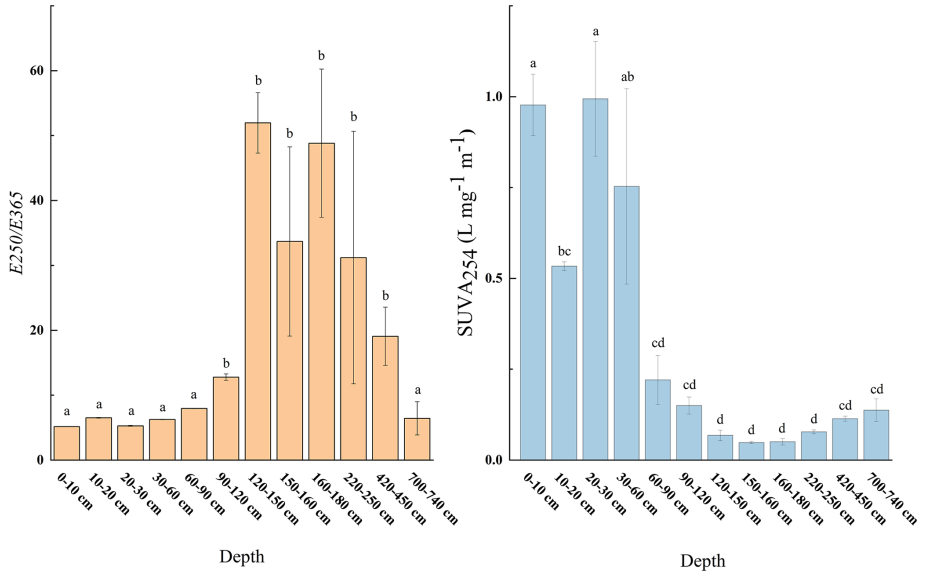

Figure 3. *E250 / E365* and $SUVA_{254}$ at different depths. Different letters represent significant differences among different sampling points ($n = 3$, $p < 0.05$), error bars represent the standard error.

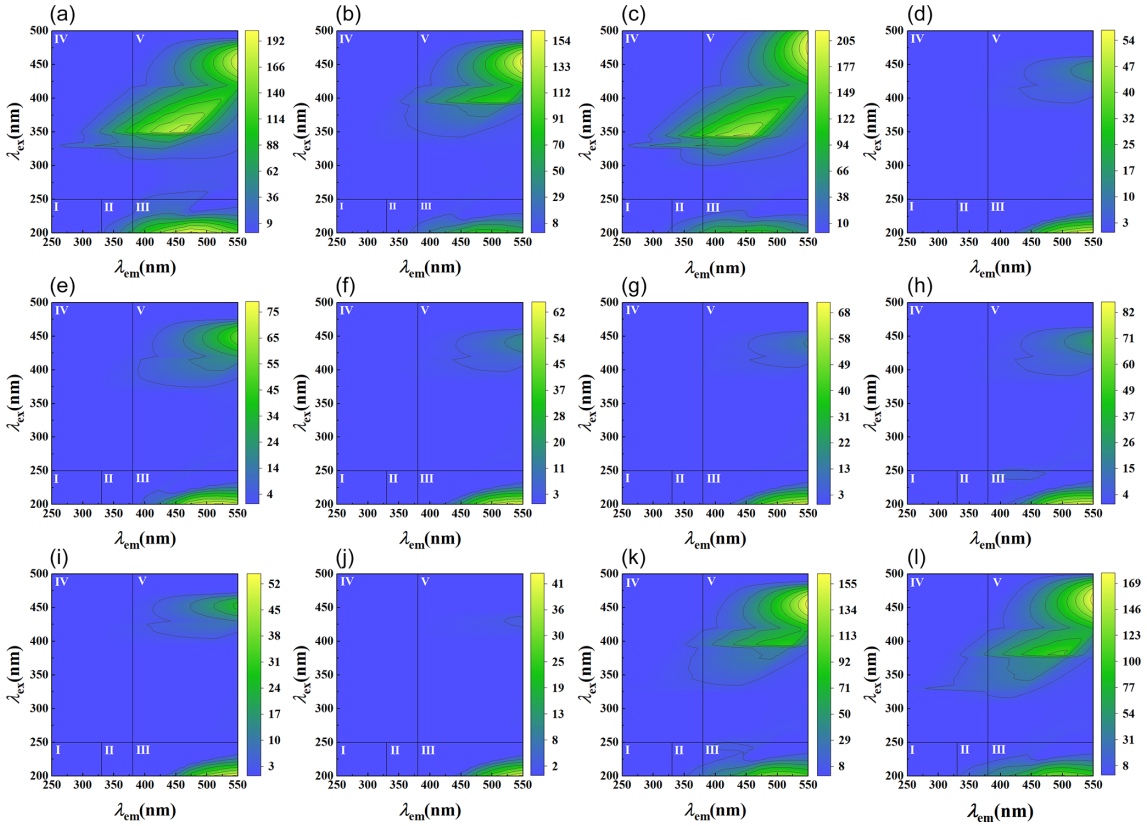

Figure 4. EEM fluorescence spectra of WSOM at different depths. Regions I, II, III, IV, and V are, respectively, for tyrosine-like aromatic protein, tryptophan-like aromatic protein, fulvic acid-like matter, soluble microbial byproduct-like matter, and humic acid-like matter. **(a)** (0–10 cm); **(b)** (10–20 cm); **(c)** (20–30 cm); **(d)** (30–60 cm); **(e)** (60–90 cm); **(f)** (90–120 cm); **(g)** (120–150 cm); **(h)** (150–160 cm); **(i)** (160–180 cm); **(j)** (220–250 cm); **(k)** (420–450 cm); **(l)** (700–740 cm).

Table 2. Content of BWSOC, BWSOC (%), reaction kinetics constant (k), and coefficient of determination (R^2) at different soil depths.

Depth	BWSOC ($g\,kg^{-1}$)	BWSOC %	k (d^{-1})	R^2
0–10 cm	0.089 ± 0.009	72.96 ± 13.41 %	0.0497	0.9394
10–20 cm	0.159 ± 0.014	81.68 ± 9.18 %	0.4991	0.7484
20–30 cm	0.127 ± 0.011	90.43 ± 0.55 %	0.1302	0.8735
30–60 cm	0.136 ± 0.064	68.08 ± 3.79 %	0.3604	0.5532
60–90 cm	0.321 ± 0.098	91.67 ± 4.14 %	1.0952	0.9847
90–120 cm	0.290 ± 0.046	95.25 ± 4.98 %	0.3651	0.9360
120–150 cm	0.285 ± 0.052	90.45 ± 5.05 %	0.1394	0.8549
150–160 cm	0.306 ± 0.025	94.54 ± 2.32 %	0.0601	0.8823
160–180 cm	0.311 ± 0.040	88.21 ± 5.45 %	0.0737	0.9058
220–250 cm	0.215 ± 0.026	73.46 ± 1.31 %	0.0863	0.8910
420–450 cm	0.101 ± 0.017	80.66 ± 1.55 %	0.0712	0.9747
700–740 cm	0.116 ± 0.045	88.25 ± 2.81 %	0.0681	0.8692

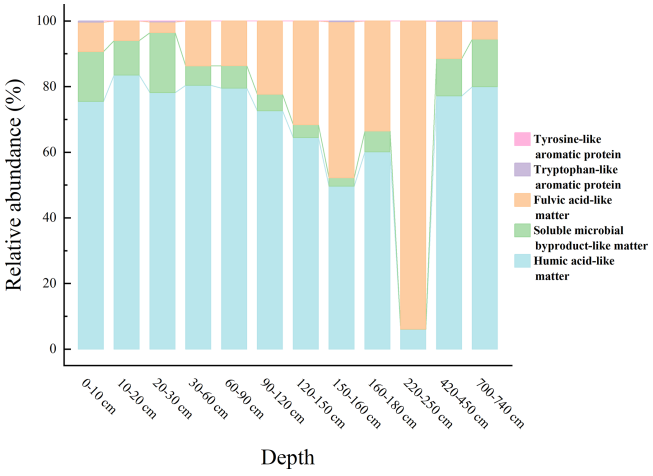

Figure 5. The EEM fluorescence spectra of WSOC at different depths

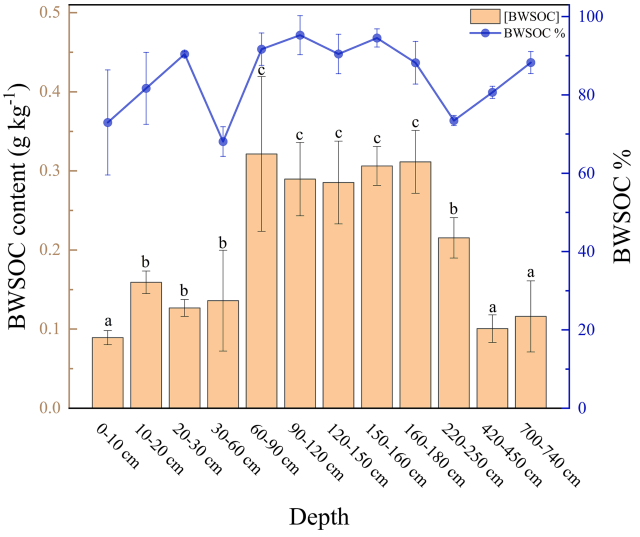

Figure 6. Content of biodegradable water-soluble organic carbon (BWSOC) and the percentage of biodegradable water-soluble organic carbon (BWSOC%) at different depths, error bars represent the standard error ($n = 3$).

content reduces the potential for SOC preservation (Bucka et al., 2023), resulting in lower WSOC concentrations in deeper layers.

We found that the WSOC in the 0–60 cm soil layer exhibited stronger aromaticity and larger molecular weight. Three-dimensional fluorescence spectroscopy confirmed that the WSOC in the surface layer was primarily composed of larger molecular humic substances, which aligns with previous findings from boreal forests in Alaska (Wickland et al., 2007). These substances are primarily plant-derived (Walker et al., 2013; Mann et al., 2016) and are often associated with root exudates and microbial exometabolites abundant in the upper soil horizons (Raudina et al., 2017).

Deep soils exhibited a higher proportion of fulvic-like substances in their WSOC, characterized by smaller molecular weights and lower aromaticity. This finding suggests that WSOC in deeper layers generally possesses lower aromaticity and molecular weight (Fouché et al., 2020). Although SOC in deep soils is usually considered has high fresh organic materials due to the low temperature limits the microbial decomposition (Heffernan et al., 2024), our results suggest that long term accumulation of highly decomposed organic matter that forms low-molecular-weight fulvic acid-like substances with lower aromaticity is still abundant in deep soils (Corvasce et al., 2006; Lv et al., 2020). This mechanism helps explain the observed decrease in WSOC aromaticity and molecular weight with increasing soil depth (Koven et al., 2015; Panneer Selvam et al., 2017; Drake et al., 2015).

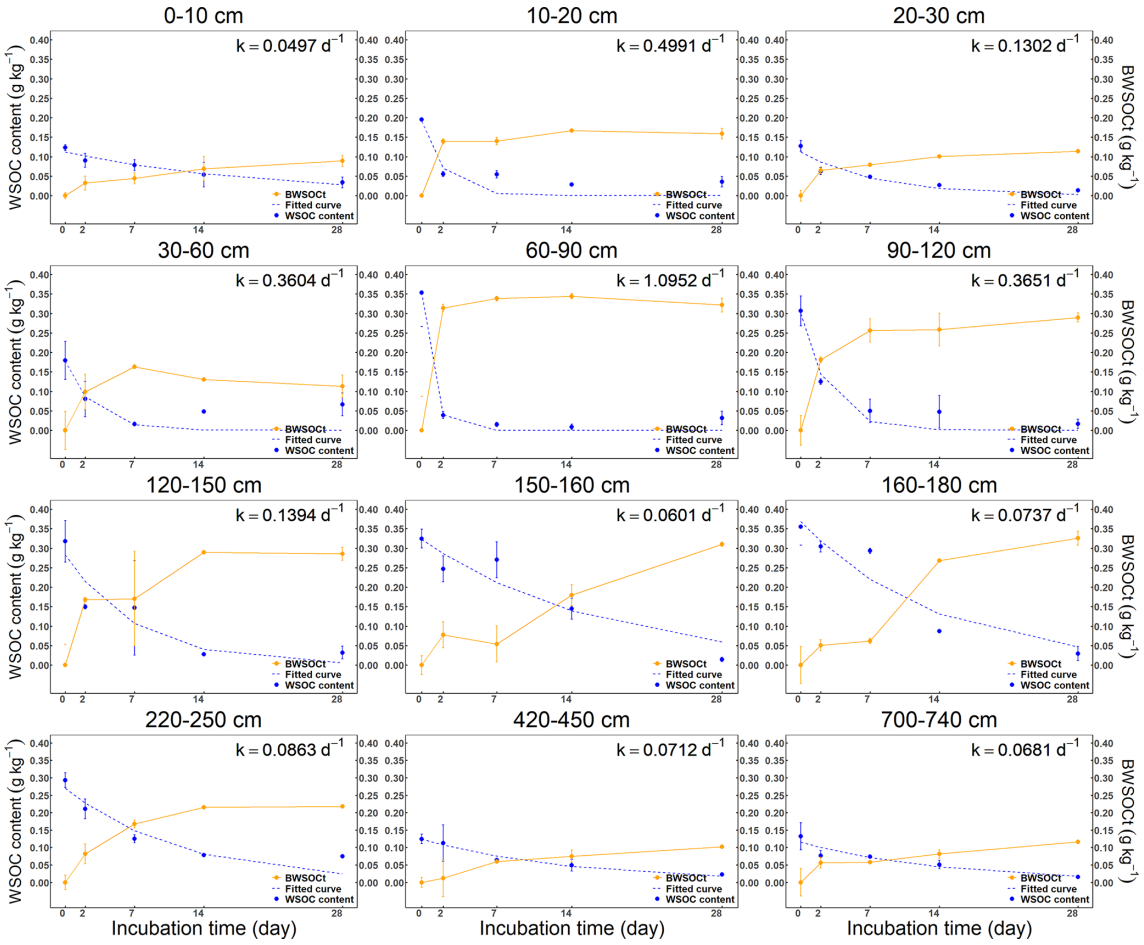

Figure 7. Water-soluble organic carbon content during the 28 d incubation at various depths. The blue curve is a nonlinear exponential fitting of WSOC content. The red curve illustrates the changes in biodegradable water-soluble organic carbon (BWSOC), with the *k*-value representing the reaction kinetics constant, error bars represent the standard error ($n = 3$).

4.2 Biodegradable water-soluble organic carbon, and the reaction kinetics constant *k*

Water-soluble organic carbon (WSOC) in boreal forest soils is highly biodegradable, with the largest proportion of biodegradable WSOC consistently occurring at depths of 60–160 cm. This depth-dependent pattern was reproduced in all replicates. In this study, the 60–160 cm interval has a buried organic horizon that contains high organic-matter concentrations (Werdin-Pfisterer et al., 2012). Spectroscopic results further confirm that the depth-related differences in BWSOC% arise from variations in the chemical composition of water-extractable organic matter. In Alaskan Kolyma River basin, WSOC concentrations decreased by about 50 % following a seven-day incubation (Spencer et al., 2015); in deep soils, ancient low-molecular-weight organic acids within WSOC are rapidly mineralized, leading to a ∼53 % decline in WSOC after 200 h of incubation (Koven et al., 2015). The high biodegradability of WSOC is closely related to its chemical composition (Burd et al., 2020). In these regions, WSOC primarily consists of low-aromaticity, low-molecular-weight organic matter that is readily decomposed by microbes (Drake et al., 2015), making it easily accessible for microbial utilization (Ward and Cory, 2015).

Despite the high biodegradability of WSOC, decomposition rates in the deeper soils (220–740 cm) were slower than those in the upper layers (0–180 cm), particularly during the later stages of incubation. This pattern suggests that microbes rapidly consumed the most bioavailable compounds in the deeper layers at the beginning of the incubation (Wild et al., 2014). Over time, the WSOC became increasingly aromatic, indicating that microbes had preferentially utilized the more easily decomposable organic matter early on (Drake et al., 2015). At 60–90 cm, WSOC had lower aromaticity and molecular weight than at 0–60 cm, contributing to faster degradation (Kalbitz et al., 2003a), particularly during the first 48 h (Roehm et al., 2009). However, degradation rates declined with depth, likely because microbial abundance and activity also were lower in deeper horizons (Marschner and Kalbitz, 2003; Neff and Asner, 2001; Yano et al., 2000).

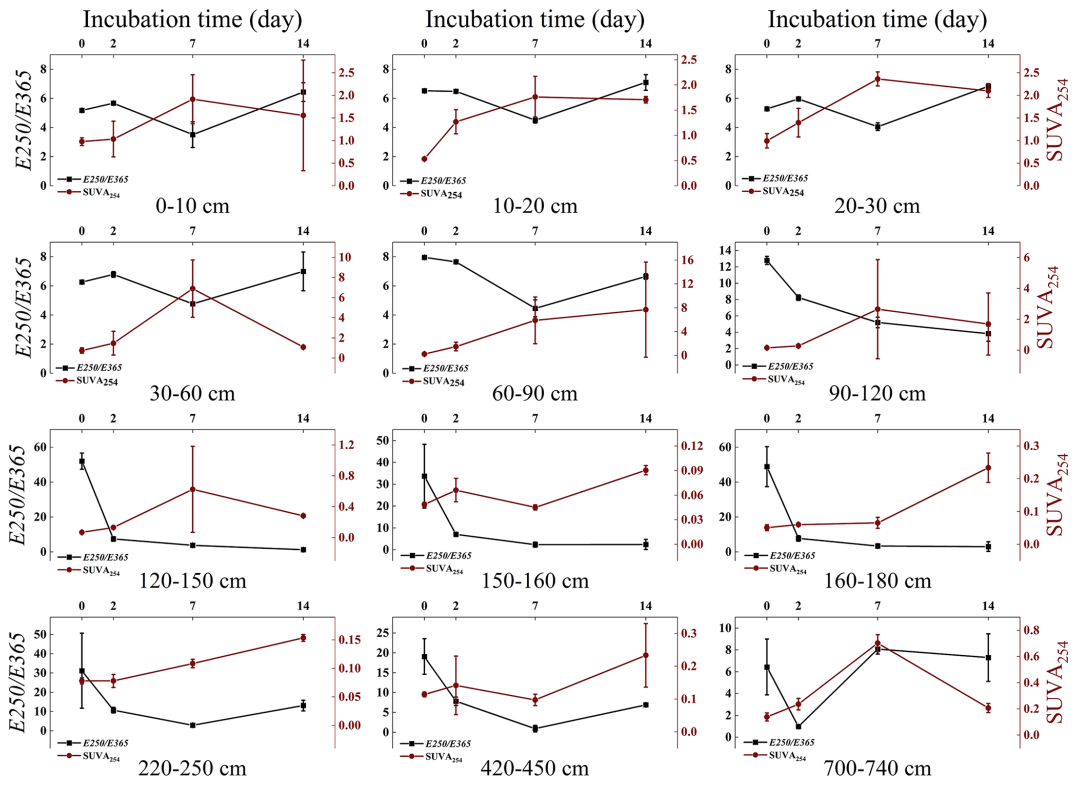

Figure 8. Water soluble organic carbon *E250 / E365* and $SUVA_{254}$ during the 14 d of incubation at different soil depths, error bars represent the standard error.

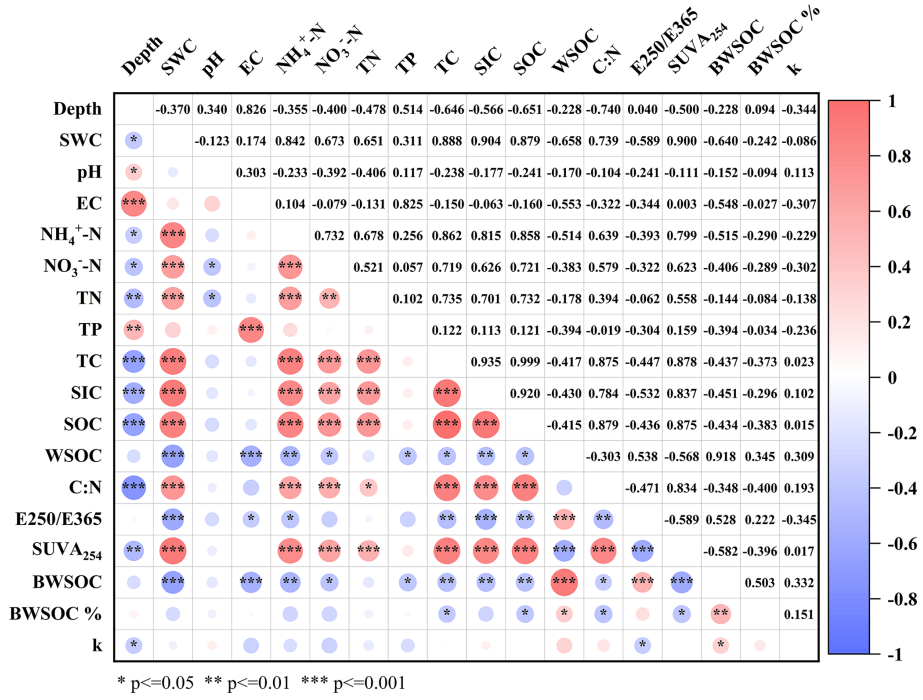

Figure 9. Correlation coefficients among different environmental factors ($n = 12$). Red indicates a positive correlation, while blue indicates a negative correlation. The deeper the color, the stronger the correlation. The color gradient ranges from −1 (complete negative correlation) to +1 (complete positive correlation).

Our study highlights the differences in the biodegradability of WSOC at various soil depths in boreal forest ecosystems. However, it is important to note that the high values of biodegradable WSOC (BWSOC) and BWSOC (%) observed in this study may be influenced by several methodological factors (Dutta et al., 2006; Vonk et al., 2015; Abbott et al., 2014; Kaplan and Newbold, 1995; Frías et al., 1995). In our study, nutrient amendments were used, and the samples were incubated under aerobic conditions at a constant temperature of 20 °C in the dark. Uniform nutrient supply could have induced nutrient-saturation effects in the 0–60 cm samples, where the C/N ratio is likely close to the Redfield ratio, thereby lowering BWSOC% (Aber, 1992; Aber et al., 1997; Gress et al., 2007). Moreover, we used depth-matched inocula to preserve native microbe–substrate interactions, consistent with previous WSOC-biodegradability studies (Bhattacharyya et al., 2022; Pei et al., 2025; Vonk et al., 2015), while we did not quantify microbial abundance or community composition. Therefore, the high BWSOC% values reflect potential rather than in-situ decomposition rates. Future work is required to examine in-situ nutrient status, microbial mass and microbial community structure to better understanding the depth-dependent WSOC dynamics.

4.3 Water-soluble organic carbon biodegradation and physicochemical parameters

BWSOC in this study showed a negative correlation with physicochemical parameters. Similar negative EC–BWSOC patterns have been reported for coastal wetland soils, where rising salinity restrained microbial residue accumulation and SOC turnover (Qu et al., 2018; Shao et al., 2022b), and laboratory studies suggest that osmotic stress can curb microbial respiration of labile dissolved organic carbon (Yang et al., 2018). Nutrient effects are strongly context dependent; for instance, nitrogen enrichment reduced soil-carbon mineralization in incubation experiments with cropland and grassland soils (Perveen et al., 2019), whereas field fertilization in a boreal forest increased DOC concentrations under nitrate addition (Shi et al., 2019). These contrasting findings indicate that multiple, site-specific processes including osmotic stress, stoichiometric imbalance, shifts in microbial community composition, or sorption dynamics may underlie the correlations observed in this study. Further manipulation experiments are required to disentangle these mechanisms.

A significant correlation was also observed between BWSOC and both $SUVA_{254}$ and the *E250 / E365* ratio. These results highlight the importance of WSOC properties in determining its biodegradability (Kalbitz et al., 2003b; Fellman et al., 2008). The composition of WSOC is influenced by physicochemical parameters such as total carbon, total nitrogen, total phosphorus, and pH (Li et al., 2018; Roth et al., 2019). The strong positive correlation between these physicochemical parameters and $SUVA_{254}$ and *E250 / E365* can be attributed to the high concentration of nutrients, which promotes the accumulation and transformation of organic matter, leading to the formation of more complex and recalcitrant organic compounds (Takaki et al., 2022).

5 Conclusion

This study quantitatively analyzed the biodegradability of water-soluble organic carbon (WSOC) at various depths in a boreal forest. Our results show that BWSOC content ranges from 0.089 to 0.321 $g\,kg^{-1}$, with the lowest observed biodegradability in surface soil WSOC still reaching 68.08 %. Three-dimensional fluorescence spectroscopy indicated that surface WEOM is dominated by highly aromatic, humic-acid-like matter. With increasing depth, the proportion of fulvic-acid-like compounds rose, whereas WSOC aromaticity and molecular weight declined. As a result, biodegradability in soils below 2 m reached 80.8 %. Although WSOC in deep horizons degraded more slowly than in the upper profile, it remained highly biodegradable. Correlation analyses further indicate that the molecular composition of WSOC is a key factor influencing its biodegradability. Overall, WSOC contents at the southern margin of the boreal forest were comparable to those reported at higher latitudes. Because WSOC represents the most labile fraction of the soil organic carbon pool, our results suggest that continued climate warming could accelerate losses of labile SOC throughout the soil profile in boreal forests.

Data availability. Data will be made available on request.

Supplement. The supplement related to this article is available online at https://doi.org/10.5194/soil-11-793-2025-supplement.

Author contributions. YZ: Conceptualization, Formal analysis, Investigation, Methodology, Writing – original draft. CL: Supervision, Resources. RL: Resources. HW: Validation, Resources. XW: Resources, Funding acquisition. ZZ: Investigation. SZ: Project administration, Data curation, Funding acquisition. XW: Writing – review and editing, Validation, Project administration.

Competing interests. The contact author has declared that none of the authors has any competing interests.

Disclaimer. Publisher's note: Copernicus Publications remains neutral with regard to jurisdictional claims made in the text, published maps, institutional affiliations, or any other geographical representation in this paper. While Copernicus Publications makes every effort to include appropriate place names, the final responsibility lies with the authors. Also, please note that this paper has not received English language copy-editing. Views expressed in the text are those of the authors and do not necessarily reflect the views of the publisher.

Acknowledgements. We sincerely thank Defu Zou, Guojie Hu, and their colleagues for their invaluable assistance with sample collection.

Financial support. This research has been supported by the Science & Technology Fundamental Resources Investigation Program (grant no. 2022FY100701), National Natural Science Foundation of China (grant nos. 42430412 and 32061143032), Basic scientific research business expenses of colleges and universities in Heilongjiang Province (grant no. 2022KYYWF0181), Harbin Normal University Postgraduate Innovation Program (grant no. HSDSSCX2022108).

Review statement. This paper was edited by Axel Don and reviewed by two anonymous referees.

References

Abbott, B. W., Larouche, J. R., Jones, J. B., Bowden, W. B., and Balser, A. W.: Elevated dissolved organic carbon biodegradability from thawing and collapsing permafrost, Journal of Geophysical Research: Biogeosciences, 119, 2049–2063, https://doi.org/10.1002/2014jg002678, 2014.

Aber, J. D.: Nitrogen cycling and nitrogen saturation in temperate forest ecosystems, Trends in Ecology & Evolution, 7, 220–224, https://doi.org/10.1016/0169-5347(92)90048-G, 1992.

Aber, J. D., Ollinger, S. V., and Driscoll, C. T.: Modeling nitrogen saturation in forest ecosystems in response to land use and atmospheric deposition, Ecological Modelling, 101, 61–78, https://doi.org/10.1016/S0304-3800(97)01953-4, 1997.

Adamczyk, B.: How do boreal forest soils store carbon?, BioEssays, 43, 2100010, https://doi.org/10.1002/bies.202100010, 2021.

Anumol, T., Sgroi, M., Park, M., Roccaro, P., and Snyder, S. A.: Predicting trace organic compound breakthrough in granular activated carbon using fluorescence and UV absorbance as surrogates, Water Research, 76, 76–87, https://doi.org/10.1016/j.watres.2015.02.019, 2015.

Bhattacharyya, S. S., Ros, G. H., Furtak, K., Iqbal, H. M. N., and Parra-Saldívar, R.: Soil carbon sequestration – An interplay between soil microbial community and soil organic matter dynamics, Science of The Total Environment, 815, https://doi.org/10.1016/j.scitotenv.2022.152928, 2022.

Bockheim, J. G.: Permafrost distribution in the southern circumpolar region and its relation to the environment: A review and recommendations for further research, Permafrost and Periglacial Processes, 6, 27–45, https://doi.org/10.1002/ppp.3430060105, 2006.

Bockheim, J. G. and Hinkel, K. M.: The Importance of "Deep" Organic Carbon in Permafrost-Affected Soils of Arctic Alaska, Soil Science Society of America Journal, 71, 1889–1892, https://doi.org/10.2136/sssaj2007.0070N, 2007.

Bond-Lamberty, B., Peckham, S. D., Ahl, D. E., and Gower, S. T.: Fire as the dominant driver of central Canadian boreal forest carbon balance, Nature, 450, 89–92, https://doi.org/10.1038/nature06272, 2007.

Bottomley, P. J., Angle, J. S., and Weaver, R. W. (Eds.): Methods of Soil Analysis, Part 2: Microbiological and Biochemical Properties, John Wiley & Sons, https://doi.org/10.2136/sssabookser5.2, 2020.

Bowden, W. B., Gooseff, M. N., Balser, A., Green, A., Peterson, B. J., and Bradford, J.: Sediment and nutrient delivery from thermokarst features in the foothills of the North Slope, Alaska: Potential impacts on headwater stream ecosystems, Journal of Geophysical Research: Biogeosciences, 113, https://doi.org/10.1029/2007jg000470, 2008.

Brown, J., Sidlauskas, F. J., and Delinski, G.: Circum-arctic map of permafrost and ground ice conditions, U.S. Geological Survey, https://doi.org/10.3133/cp45, 1997.

Bucka, F. B., Felde, V. J. M. N. L., Peth, S., and Kögel-Knabner, I.: Complementary effects of sorption and biochemical processing of dissolved organic matter for emerging structure formation controlled by soil texture, Journal of Plant Nutrition and Soil Science, 187, 51–62, https://doi.org/10.1002/jpln.202200391, 2023.

Burd, K., Estop-Aragonés, C., Tank, S. E., Olefeldt, D., and Naeth, M. A.: Lability of dissolved organic carbon from boreal peatlands: interactions between permafrost thaw, wildfire, and season, Canadian Journal of Soil Science, 100, 503–515, https://doi.org/10.1139/cjss-2019-0154, 2020.

Chavez-Vergara, B., Merino, A., Vázquez-Marrufo, G., and García-Oliva, F.: Organic matter dynamics and microbial activity during decomposition of forest floor under two native neotropical oak species in a temperate deciduous forest in Mexico, Geoderma, 235–236, 133–145, https://doi.org/10.1016/j.geoderma.2014.07.005, 2014.

Chen, W., Westerhoff, P., Leenheer, J. A., and Booksh, K.: Fluorescence Excitation-Emission Matrix Regional Integration to Quantify Spectra for Dissolved Organic Matter, Environmental Science & Technology, 37, 5701–5710, https://doi.org/10.1021/es034354c, 2003.

Corvasce, M., Zsolnay, A., D'Orazio, V., Lopez, R., and Miano, T. M.: Characterization of water extractable organic matter in a deep soil profile, Chemosphere, 62, 1583–1590, https://doi.org/10.1016/j.chemosphere.2005.07.065, 2006.

Cory, R. M., Crump, B. C., Dobkowski, J. A., and Kling, G. W.: Surface exposure to sunlight stimulates CO_2 release from permafrost soil carbon in the Arctic, Proceedings of the National Academy of Sciences, 110, 3429–3434, https://doi.org/10.1073/pnas.1214104110, 2013.

Drake, T. W., Wickland, K. P., Spencer, R. G. M., McKnight, D. M., and Striegl, R. G.: Ancient low–molecular-weight organic acids in permafrost fuel rapid carbon dioxide production upon thaw, Proceedings of the National Academy of Sciences, 112, 13946–13951, https://doi.org/10.1073/pnas.1511705112, 2015.

Dutta, K., Schuur, E. A. G., Neff, J. C., and Zimov, S. A.: Potential carbon release from permafrost soils of Northeastern Siberia, Global Change Biology, 12, 2336–2351, https://doi.org/10.1111/j.1365-2486.2006.01259.x, 2006.

Fellman, J. B., D'Amore, D. V., Hood, E., and Boone, R. D.: Fluorescence characteristics and biodegradability of dissolved organic matter in forest and wetland soils from coastal temperate watersheds in southeast Alaska, Biogeochemistry, 88, 169–184, https://doi.org/10.1007/s10533-008-9203-x, 2008.

Fouché, J., Christiansen, C. T., Lafrenière, M. J., Grogan, P., and Lamoureux, S. F.: Canadian permafrost stores large pools of am-

monium and optically distinct dissolved organic matter, Nature Communications, 11, 4500, https://doi.org/10.1038/s41467-020-18331-w, 2020.

Frías, J., Ribas, F., and Lucena, F.: Comparison of methods for the measurement of biodegradable organic carbon and assimilable organic carbon in water, Water Research, 29, 2785–2788, https://doi.org/10.1016/0043-1354(95)00074-U, 1995.

Gao, Z. Y., Niu, F. J., Wang, Y. B., Lin, Z. J., and Wang, W.: Suprapermafrost groundwater flow and exchange around a thermokarst lake on the Qinghai-Tibet Plateau, China, Journal of Hydrology, 593, 125882, https://doi.org/10.1016/j.jhydrol.2020.125882, 2021.

Gress, S. E., Nichols, T. D., Northcraft, C. C., and Peterjohn, W. T.: Nutrient Limitation in Soils Exhibiting Differing Nitrogen Availabilities: What Lies Beyond Nitrogen Saturation?, Ecology, 88, 119–130, https://doi.org/10.1890/0012-9658(2007)88[119:Nlised]2.0.Co;2, 2007.

Guggenberger, G. and Zech, W.: Dissolved organic carbon in forest floor leachates: simple degradation products or humic substances?, Science of The Total Environment, 152, 37–47, https://doi.org/10.1016/0048-9697(94)90549-5, 1994.

He, C., Chen, W.-M., Chen, C.-M., and Shi, Q.: Molecular transformation of dissolved organic matter in refinery wastewaters: Characterized by FT-ICR MS coupled with electrospray ionization and atmospheric pressure photoionization, Petroleum Science, 20, 590–599, https://doi.org/10.1016/j.petsci.2022.09.035, 2023.

Heffernan, L., Kothawala, D. N., and Tranvik, L. J.: Review article: Terrestrial dissolved organic carbon in northern permafrost, The Cryosphere, 18, 1443–1465, https://doi.org/10.5194/tc-18-1443-2024, 2024.

Helms, J. R., Stubbins, A., Ritchie, J. D., Minor, E. C., Kieber, D. J., and Mopper, K.: Absorption spectral slopes and slope ratios as indicators of molecular weight, source, and photobleaching of chromophoric dissolved organic matter, Limnology and Oceanography, 53, 955–969, https://doi.org/10.4319/lo.2008.53.3.0955, 2008.

Helton, A. M., Wright, M. S., Bernhardt, E. S., Poole, G. C., Cory, R. M., and Stanford, J. A.: Dissolved organic carbon lability increases with water residence time in the alluvial aquifer of a river floodplain ecosystem, Journal of Geophysical Research: Biogeosciences, 120, 693–706, https://doi.org/10.1002/2014JG002832, 2015.

Henneron, L., Balesdent, J., Alvarez, G., Barré, P., Baudin, F., Basile-Doelsch, I., Cécillon, L., Fernandez-Martinez, A., Hatté, C., and Fontaine, S.: Bioenergetic control of soil carbon dynamics across depth, Nature Communications, 13, https://doi.org/10.1038/s41467-022-34951-w, 2022.

Hu, G., Fang, H., Liu, G., Zhao, L., Wu, T., Li, R., and Wu, X.: Soil carbon and nitrogen in the active layers of the permafrost regions in the Three Rivers' Headstream, Environmental Earth Sciences, 72, 5113–5122, https://doi.org/10.1007/s12665-014-3382-7, 2014.

Huang, W., Deng, X., Lin, Y., and Jiang, Q. O.: An Econometric Analysis of Causes of Forestry Area Changes in Northeast China, Procedia Environmental Sciences, 2, 557–565, https://doi.org/10.1016/j.proenv.2010.10.060, 2010.

Jiang, H., Apps, M. J., Peng, C., Zhang, Y., and Liu, J.: Modelling the influence of harvesting on Chinese boreal forest carbon dynamics, Forest Ecology and Management, 169, 65–82, https://doi.org/10.1016/s0378-1127(02)00299-2, 2002.

Jones, D. and Willett, V.: Experimental evaluation of methods to quantify dissolved organic nitrogen (DON) and dissolved organic carbon (DOC) in soil, Soil Biology and Biochemistry, 38, 991–999, https://doi.org/10.1016/j.soilbio.2005.08.012, 2006.

Kaiser, K. and Kalbitz, K.: Cycling downwards – dissolved organic matter in soils, Soil Biology and Biochemistry, 52, 29–32, https://doi.org/10.1016/j.soilbio.2012.04.002, 2012.

Kalbitz, K., Schmerwitz, J., Schwesig, D., and Matzner, E.: Biodegradation of soil-derived dissolved organic matter as related to its properties, Geoderma, 113, 273–291, https://doi.org/10.1016/s0016-7061(02)00365-8, 2003a.

Kalbitz, K., Schwesig, D., Schmerwitz, J., Kaiser, K., Haumaier, L., Glaser, B., Ellerbrock, R., and Leinweber, P.: Changes in properties of soil-derived dissolved organic matter induced by biodegradation, Soil Biology and Biochemistry, 35, 1129–1142, https://doi.org/10.1016/s0038-0717(03)00165-2, 2003b.

Kaplan, L. A. and Newbold, J. D.: Measurement of streamwater biodegradable dissolved organic carbon with a plug-flow bioreactor, Water Research, 29, 2696–2706, https://doi.org/10.1016/0043-1354(95)00135-8, 1995.

Kasischke, E. S., Christensen, N. L., and Stocks, B. J.: Fire, Global Warming, and the Carbon Balance of Boreal Forests, Ecological Applications, 5, 437–451, https://doi.org/10.2307/1942034, 1995.

Khan, E., Babcock, R. W., Suffet, I. H., and Stenstrom, M. K.: Method development for measuring biodegradable organic carbon in reclaimed and treated wastewaters, Water Environment Research, 70, 1025–1032, https://doi.org/10.2175/106143098x123354, 1998.

Kirk, P. L.: Kjeldahl Method for Total Nitrogen, Analytical Chemistry, 22, 354–358, https://doi.org/10.1021/ac60038a038, 1950.

Kothawala, D. N., Stedmon, C. A., Muller, R. A., Weyhenmeyer, G. A., Kohler, S. J., and Tranvik, L. J.: Controls of dissolved organic matter quality: evidence from a large-scale boreal lake survey, Glob. Change Biol., 20, 1101–1114, https://doi.org/10.1111/gcb.12488, 2014.

Koven, C. D., Lawrence, D. M., and Riley, W. J.: Permafrost carbon-climate feedback is sensitive to deep soil carbon decomposability but not deep soil nitrogen dynamics, Proceedings of the National Academy of Sciences, 112, 3752–3757, https://doi.org/10.1073/pnas.1415123112, 2015.

Kurashev, D. G., Manasypov, R. M., Raudina, T. V., Krickov, I. V., Lim, A. G., and Pokrovsky, O. S.: Dissolved organic matter quality in thermokarst lake water and sediments across a permafrost gradient, Western Siberia, Environmental Research, 252, https://doi.org/10.1016/j.envres.2024.119115, 2024.

Li, H., Van den Bulcke, J., Wang, X., Gebremikael, M. T., Hagan, J., De Neve, S., and Sleutel, S.: Soil texture strongly controls exogenous organic matter mineralization indirectly via moisture upon progressive drying – Evidence from incubation experiments, Soil Biology and Biochemistry, 151, 108051, https://doi.org/10.1016/j.soilbio.2020.108051, 2020.

Li, K.-Y., Zhao, Y.-Y., Yuan, X.-L., Zhao, H.-B., Wang, Z.-H., Li, S.-X., and Malhi, S. S.: Comparison of Factors Affecting Soil Nitrate Nitrogen and Ammonium Nitrogen Extraction, Communications in Soil Science and Plant Analysis, 43, 571–588, https://doi.org/10.1080/00103624.2012.639108, 2012.

Li, X.-M., Chen, Q.-L., He, C., Shi, Q., Chen, S.-C., Reid, B. J., Zhu, Y.-G., and Sun, G.-X.: Organic Carbon Amendments Affect the Chemodiversity of Soil Dissolved Organic Matter and Its Associations with Soil Microbial Communities, Environmental Science & Technology, 53, 50–59, https://doi.org/10.1021/acs.est.8b04673, 2018.

Liang, G., Stefanski, A., Eddy, W. C., Bermudez, R., Montgomery, R. A., Hobbie, S. E., Rich, R. L., and Reich, P. B.: Soil respiration response to decade-long warming modulated by soil moisture in a boreal forest, Nature Geoscience, 17, 905–911, https://doi.org/10.1038/s41561-024-01512-3, 2024.

Logozzo, L. A., Martin, J. W., McArthur, J., and Raymond, P. A.: Contributions of Fe(III) to UV–Vis absorbance in river water: a case study on the Connecticut River and argument for the systematic tandem measurement of Fe(III) and CDOM, Biogeochemistry, 160, 17–33, https://doi.org/10.1007/s10533-022-00937-5, 2022.

Lv, J., Han, R., Luo, L., Zhang, X., and Zhang, S.: A Novel Strategy to Evaluate the Aromaticity Degree of Natural Organic Matter Based on Oxidization-Induced Chemiluminescence, Environmental Science & Technology, 54, 4171–4179, https://doi.org/10.1021/acs.est.9b07499, 2020.

Lv, S., Liu, R., Guo, Z., and Wang, S.: Characteristics of soil aggregate distribution and organic carbon mineralization in quinoa fields with different soil textures in the northern of the Yinshan Mountains in inner Mongolia, Frontiers in Environmental Science, 12, https://doi.org/10.3389/fenvs.2024.1494983, 2024.

Ma, Q., Jin, H., Yu, C., and Bense, V. F.: Dissolved organic carbon in permafrost regions: A review, Science China Earth Sciences, 62, 349–364, https://doi.org/10.1007/s11430-018-9309-6, 2019.

Mann, P. J., Spencer, R. G. M., Hernes, P. J., Six, J., Aiken, G. R., Tank, S. E., McClelland, J. W., Butler, K. D., Dyda, R. Y., and Holmes, R. M.: Pan-Arctic Trends in Terrestrial Dissolved Organic Matter from Optical Measurements, Frontiers in Earth Science, 4, https://doi.org/10.3389/feart.2016.00025, 2016.

Margesin, R.: Permafrost soils, Springer Science & Business Media, https://doi.org/10.1007/978-3-540-69371-0, 2008.

Marschner, B. and Kalbitz, K.: Controls of bioavailability and biodegradability of dissolved organic matter in soils, Geoderma, 113, 211–235, https://doi.org/10.1016/s0016-7061(02)00362-2, 2003.

Mehring, A., Lowrance, R., Helton, A., Pringle, C., Thompson, A., Bosch, D., and Vellidis, G.: Interannual drought length governs dissolved organic carbon dynamics in blackwater rivers of the western upper Suwannee River basin, Journal of Geophysical Research: Biogeosciences, 118, 1636–1645, https://doi.org/10.1002/2013JG002415, 2013.

Mentges, M. I., Reichert, J. M., Rodrigues, M. F., Awe, G. O., and Mentges, L. R.: Capacity and intensity soil aeration properties affected by granulometry, moisture, and structure in no-tillage soils, Geoderma, 263, 47–59, https://doi.org/10.1016/j.geoderma.2015.08.042, 2016.

Michalzik, B., Tipping, E., Mulder, J., Lancho, J. F. G., Matzner, E., Bryant, C. L., Clarke, N., Lofts, S., and Esteban, M. A. V.: Modelling the production and transport of dissolved organic carbon in forest soils, Biogeochemistry, 66, 241–264, https://doi.org/10.1023/b:Biog.0000005329.68861.27, 2003.

Moore, T. R.: Dissolved organic carbon in a northern boreal landscape, Global Biogeochemical Cycles, 17, https://doi.org/10.1029/2003gb002050, 2003.

Mu, C. C., Abbott, B. W., Wu, X. D., Zhao, Q., Wang, H. J., Su, H., Wang, S. F., Gao, T. G., Guo, H., Peng, X. Q., and Zhang, T. J.: Thaw Depth Determines Dissolved Organic Carbon Concentration and Biodegradability on the Northern Qinghai-Tibetan Plateau, Geophysical Research Letters, 44, 9389–9399, https://doi.org/10.1002/2017gl075067, 2017.

Murphy, K. R., Stedmon, C. A., Waite, T. D., and Ruiz, G. M.: Distinguishing between terrestrial and autochthonous organic matter sources in marine environments using fluorescence spectroscopy, Marine Chemistry, 108, 40–58, https://doi.org/10.1016/j.marchem.2007.10.003, 2008.

Neff, J. C. and Asner, G. P.: Dissolved Organic Carbon in Terrestrial Ecosystems: Synthesis and a Model, Ecosystems, 4, 29–48, https://doi.org/10.1007/s100210000058, 2001.

Nelson, D. W. and Sommers, L. E.: Total Carbon, Organic Carbon, and Organic Matter, Methods of Soil Analysis, 961–1010, https://doi.org/10.2136/sssabookser5.3.c34, 1996.

Ohlson, M., Dahlberg, B., Økland, T., Brown, K. J., and Halvorsen, R.: The charcoal carbon pool in boreal forest soils, Nature Geoscience, 2, 692–695, https://doi.org/10.1038/ngeo617, 2009.

Olefeldt, D. and Roulet, N. T.: Effects of permafrost and hydrology on the composition and transport of dissolved organic carbon in a subarctic peatland complex, Journal of Geophysical Research: Biogeosciences, 117, https://doi.org/10.1029/2011jg001819, 2012.

Olefeldt, D., Persson, A., and Turetsky, M. R.: Influence of the permafrost boundary on dissolved organic matter characteristics in rivers within the Boreal and Taiga plains of western Canada, Environmental Research Letters, 9, https://doi.org/10.1088/1748-9326/9/3/035005, 2014.

Öquist, M. G., Bishop, K., Grelle, A., Klemedtsson, L., Köhler, S. J., Laudon, H., Lindroth, A., Ottosson Löfvenius, M., Wallin, M. B., and Nilsson, M. B.: The Full Annual Carbon Balance of Boreal Forests Is Highly Sensitive to Precipitation, Environmental Science & Technology Letters, 1, 315–319, https://doi.org/10.1021/ez500169j, 2014.

Panneer Selvam, B., Laudon, H., Guillemette, F., and Berggren, M.: Influence of soil frost on the character and degradability of dissolved organic carbon in boreal forest soils, Journal of Geophysical Research: Biogeosciences, 121, 829–840, https://doi.org/10.1002/2015jg003228, 2016.

Panneer Selvam, B., Lapierre, J.-F., Guillemette, F., Voigt, C., Lamprecht, R. E., Biasi, C., Christensen, T. R., Martikainen, P. J., and Berggren, M.: Degradation potentials of dissolved organic carbon (DOC) from thawed permafrost peat, Scientific Reports, 7, 45811, https://doi.org/10.1038/srep45811, 2017.

Paré, M. C. and Bedard-Haughn, A.: Soil organic matter quality influences mineralization and GHG emissions in cryosols: a field-based study of sub- to high Arctic, Global Change Biology, 19, 1126–1140, https://doi.org/10.1111/gcb.12125, 2013.

Park, M. and Snyder, S. A.: Sample handling and data processing for fluorescent excitation-emission matrix (EEM) of dissolved organic matter (DOM), Chemosphere, 193, 530-537, https://doi.org/10.1016/j.chemosphere.2017.11.069, 2018.

Pei, J., Li, J., Luo, Y., Rillig, M. C., Smith, P., Gao, W., Li, B., Fang, C., and Nie, M.: Patterns and drivers of soil microbial car-

bon use efficiency across soil depths in forest ecosystems, Nature Communications, 16, https://doi.org/10.1038/s41467-025-60594-8, 2025.

Peng, R., Liu, H., Anenkhonov, O. A., Sandanov, D. V., Korolyuk, A. Y., Shi, L., Xu, C., Dai, J., and Wang, L.: Tree growth is connected with distribution and warming-induced degradation of permafrost in southern Siberia, Global Change Biology, 28, 5243–5253, https://doi.org/10.1111/gcb.16284, 2022.

Pengerud, A., Cécillon, L., Johnsen, L. K., Rasse, D. P., and Strand, L. T.: Permafrost Distribution Drives Soil Organic Matter Stability in a Subarctic Palsa Peatland, Ecosystems, 16, 934–947, https://doi.org/10.1007/s10021-013-9652-5, 2013.

Perveen, N., Ayub, M., Shahzad, T., Siddiq, M. R., Memon, M. S., Barot, S., Saeed, H., and Xu, M.: Soil carbon mineralization in response to nitrogen enrichment in surface and subsurface layers in two land use types, PeerJ, 7, e7130, https://doi.org/10.7717/peerj.7130, 2019.

Peuravuori, J. and Pihlaja, K.: Preliminary Study of Lake Dissolved Organic Matter in Light of Nanoscale Supramolecular Assembly, Environmental Science & Technology, 38, 5958–5967, https://doi.org/10.1021/es0400411, 2004.

Ping, C. L., Jastrow, J. D., Jorgenson, M. T., Michaelson, G. J., and Shur, Y. L.: Permafrost soils and carbon cycling, SOIL, 1, 147–171, https://doi.org/10.5194/soil-1-147-2015, 2015.

Qu, W., Li, J., Han, G., Wu, H., Song, W., and Zhang, X.: Effect of salinity on the decomposition of soil organic carbon in a tidal wetland, Journal of Soils and Sediments, 19, 609–617, https://doi.org/10.1007/s11368-018-2096-y, 2018.

Ran, Y., Li, X., Cheng, G., Zhang, T., Wu, Q., Jin, H., and Jin, R.: Distribution of Permafrost in China: An Overview of Existing Permafrost Maps, Permafrost and Periglacial Processes, 23, 322–333, https://doi.org/10.1002/ppp.1756, 2012.

Randerson, J. T., Liu, H., Flanner, M. G., Chambers, S. D., Jin, Y., Hess, P. G., Pfister, G., Mack, M. C., Treseder, K. K., Welp, L. R., Chapin, F. S., Harden, J. W., Goulden, M. L., Lyons, E., Neff, J. C., Schuur, E. A., and Zender, C. S.: The impact of boreal forest fire on climate warming, Science, 314, 1130–1132, https://doi.org/10.1126/science.1132075, 2006.

Raudina, T. V., Loiko, S. V., Lim, A. G., Krickov, I. V., Shirokova, L. S., Istigechev, G. I., Kuzmina, D. M., Kulizhsky, S. P., Vorobyev, S. N., and Pokrovsky, O. S.: Dissolved organic carbon and major and trace elements in peat porewater of sporadic, discontinuous, and continuous permafrost zones of western Siberia, Biogeosciences, 14, 3561–3584, https://doi.org/10.5194/bg-14-3561-2017, 2017.

Reynolds, S.: The gravimetric method of soil moisture determination Part IA study of equipment, and methodological problems, Journal of Hydrology, 11, 258–273, 1970.

Roehm, C. L., Giesler, R., and Karlsson, J.: Bioavailability of terrestrial organic carbon to lake bacteria: The case of a degrading subarctic permafrost mire complex, Journal of Geophysical Research, 114, https://doi.org/10.1029/2008jg000863, 2009.

Roth, V.-N., Lange, M., Simon, C., Hertkorn, N., Bucher, S., Goodall, T., Griffiths, R. I., Mellado-Vázquez, P. G., Mommer, L., Oram, N. J., Weigelt, A., Dittmar, T., and Gleixner, G.: Persistence of dissolved organic matter explained by molecular changes during its passage through soil, Nature Geoscience, 12, 755–761, https://doi.org/10.1038/s41561-019-0417-4, 2019.

Scaglia, B. and Adani, F.: Biodegradability of soil water soluble organic carbon extracted from seven different soils, Journal of Environmental Sciences, 21, 641–646, https://doi.org/10.1016/s1001-0742(08)62319-0, 2009.

Schirrmeister, L., Kunitsky, V., Grosse, G., Wetterich, S., Meyer, H., Schwamborn, G., Babiy, O., Derevyagin, A., and Siegert, C.: Sedimentary characteristics and origin of the Late Pleistocene Ice Complex on north-east Siberian Arctic coastal lowlands and islands – A review, Quaternary International, 241, 3–25, https://doi.org/10.1016/j.quaint.2010.04.004, 2011.

Schuur, E. A. G., Abbott, B. W., Commane, R., Ernakovich, J., Euskirchen, E., Hugelius, G., Grosse, G., Jones, M., Koven, C., Leshyk, V., Lawrence, D., Loranty, M. M., Mauritz, M., Olefeldt, D., Natali, S., Rodenhizer, H., Salmon, V., Schädel, C., Strauss, J., Treat, C., and Turetsky, M.: Permafrost and climate change: Carbon cycle feedbacks from the warming Arctic, Annual Review of Environment and Resources, 47, 343–371, https://doi.org/10.1146/annurev-environ-012220-011847, 2022.

Semenov, P., Pismeniuk, A., Kil, A., Shatrova, E., Belova, N., Gromov, P., Malyshev, S., He, W., Lodochnikova, A., Tarasevich, I., Streletskaya, I., and Leibman, M.: Characterizing Dissolved Organic Matter and Other Water-Soluble Compounds in Ground Ice of the Russian Arctic: A Focus on Ground Ice Classification within the Carbon Cycle Context, Geosciences, 14, https://doi.org/10.3390/geosciences14030077, 2024.

Sgroi, M., Anumol, T., Roccaro, P., Vagliasindi, F. G. A., and Snyder, S. A.: Modeling emerging contaminants breakthrough in packed bed adsorption columns by UV absorbance and fluorescing components of dissolved organic matter, Water Research, 145, 667–677, https://doi.org/10.1016/j.watres.2018.09.018, 2018.

Shao, M., Zhang, S., Niu, B., Pei, Y., Song, S., Lei, T., and Yun, H.: Soil texture influences soil bacterial biomass in the permafrost-affected alpine desert of the Tibetan plateau, Frontiers in Microbiology, 13, https://doi.org/10.3389/fmicb.2022.1007194, 2022a.

Shao, P., Han, H., Sun, J., Yang, H., and Xie, H.: Salinity Effects on Microbial Derived-C of Coastal Wetland Soils in the Yellow River Delta, Frontiers in Ecology and Evolution, 10, https://doi.org/10.3389/fevo.2022.872816, 2022b.

Shi, L., Dech, J. P., Yao, H., Zhao, P., Shu, Y., and Zhou, M.: The effects of nitrogen addition on dissolved carbon in boreal forest soils of northeastern China, Scientific Reports, 9, https://doi.org/10.1038/s41598-019-44796-x, 2019.

Song, X., Wang, G., Ran, F., Huang, K., Sun, J., and Song, C.: Soil moisture as a key factor in carbon release from thawing permafrost in a boreal forest, Geoderma, 357, https://doi.org/10.1016/j.geoderma.2019.113975, 2020.

Sparks, D. L., Page, A. L., Helmke, P. A., and Loeppert, R. H.: Methods of soil analysis, part 3: Chemical methods, John Wiley & Sons, https://doi.org/10.2136/sssabookser5.3, 2020.

Spencer, R. G. M., Mann, P. J., Dittmar, T., Eglinton, T. I., McIntyre, C., Holmes, R. M., Zimov, N., and Stubbins, A.: Detecting the signature of permafrost thaw in Arctic rivers, Geophysical Research Letters, 42, 2830–2835, https://doi.org/10.1002/2015gl063498, 2015.

Strauss, J., Schirrmeister, L., Grosse, G., Fortier, D., Hugelius, G., Knoblauch, C., Romanovsky, V., Schädel, C., Schneider von Deimling, T., Schuur, E. A. G., Shmelev, D., Ulrich, M., and Veremeeva, A.: Deep Yedoma per-

mafrost: A synthesis of depositional characteristics and carbon vulnerability, Earth-Science Reviews, 172, 75–86, https://doi.org/10.1016/j.earscirev.2017.07.007, 2017.

Sun, B., Li, Y., Song, M., Li, R., Li, Z., Zhuang, G., Bai, Z., and Zhuang, X.: Molecular characterization of the composition and transformation of dissolved organic matter during the semi-permeable membrane covered hyperthermophilic composting, Journal of Hazardous Materials, 425, https://doi.org/10.1016/j.jhazmat.2021.127496, 2022.

Takaki, Y., Hattori, K., and Yamashita, Y.: Factors Controlling the Spatial Distribution of Dissolved Organic Matter With Changes in the C/N Ratio From the Upper to Lower Reaches of the Ishikari River, Japan, Frontiers in Earth Science, 10, https://doi.org/10.3389/feart.2022.826907, 2022.

Thurman, E. M.: Organic Geochemistry of Natural Waters, Springer Science & Business Media, https://doi.org/10.1007/978-94-009-5095-5, 1985.

Uhlířová, E., Šantrůčková, H., and Davidov, S. P.: Quality and potential biodegradability of soil organic matter preserved in permafrost of Siberian tussock tundra, Soil Biology and Biochemistry, 39, 1978–1989, https://doi.org/10.1016/j.soilbio.2007.02.018, 2007.

Vonk, J. E., Tank, S. E., Mann, P. J., Spencer, R. G. M., Treat, C. C., Striegl, R. G., Abbott, B. W., and Wickland, K. P.: Biodegradability of dissolved organic carbon in permafrost soils and aquatic systems: a meta-analysis, Biogeosciences, 12, 6915–6930, https://doi.org/10.5194/bg-12-6915-2015, 2015.

Vos, C., Don, A., Prietz, R., Heidkamp, A., and Freibauer, A.: Field-based soil-texture estimates could replace laboratory analysis, Geoderma, 267, 215–219, https://doi.org/10.1016/j.geoderma.2015.12.022, 2016.

Walker, S. A., Amon, R. M. W., and Stedmon, C. A.: Variations in high-latitude riverine fluorescent dissolved organic matter: A comparison of large Arctic rivers, Journal of Geophysical Research: Biogeosciences, 118, 1689–1702, https://doi.org/10.1002/2013jg002320, 2013.

Walz, J., Knoblauch, C., Böhme, L., and Pfeiffer, E.-M.: Regulation of soil organic matter decomposition in permafrost-affected Siberian tundra soils – Impact of oxygen availability, freezing and thawing, temperature, and labile organic matter, Soil Biology and Biochemistry, 110, 34–43, https://doi.org/10.1016/j.soilbio.2017.03.001, 2017.

Ward, C. P. and Cory, R. M.: Chemical composition of dissolved organic matter draining permafrost soils, Geochimica et Cosmochimica Acta, 167, 63–79, https://doi.org/10.1016/j.gca.2015.07.001, 2015.

Weishaar, J. L., Aiken, G. R., Bergamaschi, B. A., Fram, M. S., Fujii, R., and Mopper, K.: Evaluation of specific ultraviolet absorbance as an indicator of the chemical composition and reactivity of dissolved organic carbon, Environmental Science & Technology, 37, 4702–4708, https://doi.org/10.1021/es030360x, 2003a.

Weishaar, J. L., Aiken, G. R., Bergamaschi, B. A., Fram, M. S., Fujii, R., and Mopper, K.: Evaluation of specific ultraviolet absorbance as an indicator of the chemical composition and reactivity of dissolved organic carbon, Environ. Sci. Technol., 37, 4702–4708, https://doi.org/10.1021/es030360x, 2003b.

Werdin-Pfisterer, N. R., Kielland, K., and Boone, R. D.: Buried organic horizons represent amino acid reservoirs in boreal forest soils, Soil Biology and Biochemistry, 55, 122–131, https://doi.org/10.1016/j.soilbio.2012.06.012, 2012.

Wickland, K. P., Neff, J. C., and Aiken, G. R.: Dissolved Organic Carbon in Alaskan Boreal Forest: Sources, Chemical Characteristics, and Biodegradability, Ecosystems, 10, 1323–1340, https://doi.org/10.1007/s10021-007-9101-4, 2007.

Wild, B., Schnecker, J., Alves, R. J., Barsukov, P., Barta, J., Capek, P., Gentsch, N., Gittel, A., Guggenberger, G., Lashchinskiy, N., Mikutta, R., Rusalimova, O., Santruckova, H., Shibistova, O., Urich, T., Watzka, M., Zrazhevskaya, G., and Richter, A.: Input of easily available organic C and N stimulates microbial decomposition of soil organic matter in arctic permafrost soil, Soil Biology and Biochemistry, 75, 143–151, https://doi.org/10.1016/j.soilbio.2014.04.014, 2014.

Wu, M. H., Chen, S. Y., Chen, J. W., Xue, K., Chen, S. L., Wang, X. M., Chen, T., Kang, S. C., Rui, J. P., Thies, J. E., Bardgett, R. D., and Wang, Y. F.: Reduced microbial stability in the active layer is associated with carbon loss under alpine permafrost degradation, Proceedings of the National Academy of Sciences of the United States of America, 118, e2025321118, https://doi.org/10.1073/pnas.2025321118, 2021.

Yang, J., Zhan, C., Li, Y., Zhou, D., Yu, Y., and Yu, J.: Effect of salinity on soil respiration in relation to dissolved organic carbon and microbial characteristics of a wetland in the Liaohe River estuary, Northeast China, Science of The Total Environment, 642, 946–953, 10.1016/j.scitotenv.2018.06.121, 2018.

Yano, Y., McDowell, W. H., and Aber, J. D.: Biodegradable dissolved organic carbon in forest soil solution and effects of chronic nitrogen deposition, Soil Biology and Biochemistry, 32, 1743–1751, https://doi.org/10.1016/S0038-0717(00)00092-4, 2000.

Zhang, R. V., Zabolotnik, S. I., and Zabolotnik, P. S.: Assessment of the thermal effect of large industrial buildings on permafrost foundation soils in Yakutsk, Research in Cold and Arid Regions, 15, 262–267, https://doi.org/10.1016/j.rcar.2023.12.001, 2023.

Zhang, Y., Liu, X., Li, P., Xiao, L., Zhou, S., Wang, X., and Wang, R.: Critical factors in soil organic carbon mineralization induced by drying, wetting and wet-dry cycles in a typical watershed of Loess Plateau, Journal of Environmental Management, 362, 121313, https://doi.org/10.1016/j.jenvman.2024.121313, 2024.

Zhong, S. N., Li, B., Hou, B. W., Xu, X. M., Hu, J. Y., Jia, R., Yang, S. Q., Zhou, S. G., and Ni, J. R.: Structure, stability, and potential function of groundwater microbial community responses to permafrost degradation on varying permafrost of the Qinghai-Tibet Plateau, Science of the Total Environment, 875, 162693, https://doi.org/10.1016/j.scitotenv.2023.162693, 2023.

Zhou, X., Ma, A., Chen, X., Zhang, Q., Guo, X., and Zhuang, G.: Climate Warming-Driven Changes in the Molecular Composition of Soil Dissolved Organic Matter Across Depth: A Case Study on the Tibetan Plateau, Environmental Science & Technology, 57, 16884–16894, https://doi.org/10.1021/acs.est.3c04899, 2023.

Zou, T. and Yoshino, K.: Environmental vulnerability evaluation using a spatial principal components approach in the Daxing'anling region, China, Ecological Indicators, 78, 405–415, https://doi.org/10.1016/j.ecolind.2017.03.039, 2017.